Nuclear Magnetic Relaxation and Atomic Diffusion in Aluminum Alloys*

T. J. ROWLAND AND F. Y. FRADIN†
Department of Mining, Metallurgy and Petroleum Engineering and the Materials Research Laboratory, University of Illinois, Urbana, Illinois 61801
(Received 21 November 1968)

The rotating-frame nuclear magnetic relaxation time $T_{1\rho}$ and local field H_L have been measured for Al^{27} in a series of dilute aluminum-base alloys and in pure Al. The local field in the alloys is found to include both a magnetic dipole contribution, discussed previously by Slichter *et al.*, and an electric quadrupole contribution. The latter is a direct consequence of solute perturbations of the structure and is of particular interest here. We have measured $T_{1\rho}$ between 24 and 660°C and associated it with time fluctuations of both the magnetic-dipolar and electric-quadrupolar interactions. From the magnitude and temperature dependence of the quadrupolar contribution, the solute atomic jump rate is estimated. The energy of migration for Zn, Mg, and Ag solutes is found to be much smaller than that of Al in aluminum metal.

I. INTRODUCTION

SUBSTITUTIONAL impurity diffusion in metals has been studied by a variety of macroscopic techniques[1]; however, attempts to relate the theoretically predicted activation energy for solute diffusion to the experimentally determined activation energy from mass flow experiments are complicated by correlation effects.[2,3] Nuclear-magnetic-resonance techniques have been employed to directly measure the time between atomic jumps τ in a pure metal.[4,5] Such jumps cause time-dependent fluctuations of internal fields which interact with the resonant nuclei to influence the nuclear relaxation. rates. Recently, methods have been established by Slichter and Ailion SA[6,7] for measuring the jump time over an extensive range of temperature by making use of the properties of spin-lattice relaxation in the rotating frame. In this frame a characteristic time of relaxation $T_{1\rho}$ expresses the decay time of the magnetization.

This paper reports an investagation of nuclear relaxation at elevated temperatures in some dilute aluminum-base alloys. A marked dependence of the Al^{27} relaxation time on solute concentration is shown to be a result of the fluctuating long-range electric-field gradients associated with the lattice motion of the solute atoms. We thus find that the activation energy associated with diffusional relaxation is largely determined by the activation energy for solute motion. The alloys of interest are substitutional solid solutions, and assuming the vacancy mechanism of diffusion we attempt to interpret the observed relaxation behavior in terms of the parameters characteristic of the diffusion process, namely the energies of migration of the solute and solvent atoms, the vacancy formation energy, the impurity-vacancy binding energy, and the appropriate frequency factors.

The framework for our interpretation of the data is developed in Sec. II. The relaxation rate $1/T_{1\rho}$ is expressed as the sum of electronic and diffusional contributions, the latter including both magnetic-dipolar and electric-quadrupolar interactions of the Al^{27} nuclei with the fields in the solid. The experimental procedure is briefly described in Sec. III followed in Sec. IV by a presentation and discussion of the results obtained. From the primary data the component of the relaxation caused by atomic motion is isolated and compared with the appropriate expressions from Sec. II. Conclusions comprise Sec. V.

II. PHYSICAL BASIS

A. Basic Theory

A system of spins is said to be described by a spin temperature θ, not necessarily the same as the lattice temperature θ_l, if the density operator can be written as

$$\rho=(1/Z)e^{-\mathcal{H}/k\theta}, \tag{1}$$

where

$$Z=\mathrm{Tr}e^{-\mathcal{H}/k\theta}=\sum_n e^{-E_n/k\theta}. \tag{2}$$

Tr indicates the trace is to be taken, the E_n's are the eigenvalues of the Hamiltonian $\mathcal{H}$, and k is the Boltzmann constant. Redfield[8] showed that in the presence of a rf field H_1, large enough to saturate the absorption, the system is characterized by a spin temperature in a rotating frame in which H_1 is fixed. In this frame the dominant time dependence of the nuclear Hamiltonian, that of the rf field, is removed. Thus, the most probable state of the system is a canonical distribution describable by a density matrix of the form given in Eq. (1) in which the E_n's are eigenvalues of the Hamiltonian transformed into the rotating frame.

We consider a system of nuclei interacting with an applied field H_0 and a circularly polarized rf field H_1

* This research was supported in part by the U. S. Atomic Energy Commission under Contract No. AT(11-1)-1198.
† Present address: Metallurgy Division, Argonne National Laboratory, Argonne, Ill.
[1] P. Shewmon, *Diffusion in Solids* (McGraw-Hill Book Co., New York, 1963).
[2] J. R. Manning, Phys. Rev. Letters **1**, 365 (1958).
[3] A. D. Le Claire, Phil. Mag. **7**, 141 (1962).
[4] D. F. Holcomb and R. E. Norberg, Phys. Rev. **98**, 1074 (1955).
[5] J. J. Spokas and C. P. Slichter, Phys. Rev. **113**, 1462 (1959).
[6] C. P. Slichter and D. Ailion, Phys. Rev. **135**, A1099 (1964).
[7] D. C. Ailion and C. P. Slichter, Phys. Rev. **137**, A235 (1965).
[8] A. G. Redfield, Phys. Rev. **98**, 1787 (1955).

of frequency ω. The nuclei also interact with one another through the magnetic dipole-dipole interaction and with electric-field gradients caused primarily by impurity atoms. Using the standard rotating coordinate transformation we have an effective Hamiltonian $\mathcal{H}$ in the rotating frame given by

$$\mathcal{H}=\mathcal{H}_z+\mathcal{H}_d{}^0+\mathcal{H}_q{}^0, \tag{3}$$

where the Zeeman term is given by

$$\mathcal{H}_z=-\gamma\hbar\sum_j[(H_0-(\omega/\gamma))I_{zj}+H_1I_{xj}], \tag{4}$$

the dipolar term is given by

$$\mathcal{H}_d{}^0=\tfrac{1}{4}\gamma^2\hbar^2\sum_{i,j}(3I_{zi}I_{zj}-\mathbf{I}_i\cdot\mathbf{I}_j)\left(\frac{1-3\cos^2\theta_{ij}}{R_{ij}{}^3}\right), \tag{5}$$

and the quadrupolar term is given by

$$\mathcal{H}_q{}^0=\sum_{i,k}\frac{e^2q_{ik}Q}{4I(2I-1)}(3I_{zi}{}^2-I^2)\tfrac{1}{2}(3\cos^2\phi_{ik}-1). \tag{6}$$

Here γ is the gyromagnetic ratio of the Al^{27} nucleus, $\hbar$ is Planck's constant divided by 2π, I is the dimensionless momentum operator, θ_{ij} is the angle that the internuclear vector $\mathbf{R}_{ij}$ makes with the z axis, and ϕ_{ik} is the angle that the axis of the field gradient q makes with the z axis. In Eq. (6) we have assumed the field gradient to be axially symmetric. The nonsecular terms in $\mathcal{H}$ have been dropped since they have time dependences $e^{\pm i\omega t}$ and $e^{\pm 2i\omega t}$ in the rotating frame and can be neglected.

For the case in which there is rapid transfer of energy within the spin system, one may make use of the spin temperature in the rotating frame to calculate the magnetization $\langle\mathbf{M}\rangle$ and energy E from

$$\langle\mathbf{M}\rangle=\mathrm{Tr}(\rho\mathbf{M})=\frac{C\mathbf{H}_{\mathrm{eff}}}{\theta} \tag{7}$$

and

$$E=\mathrm{Tr}(\rho\mathcal{H})=-\frac{C(H_{\mathrm{eff}}{}^2+H_D{}^2+H_Q{}^2)}{\theta}, \tag{8}$$

where

$$\mathbf{H}_{\mathrm{eff}}=(H_0-\omega/\gamma)\mathbf{k}+H_1\mathbf{i}=h_0\mathbf{k}+H_1\mathbf{i}$$

and C is the Curie constant. The dipolar contribution to the local field is given by

$$H_D{}^2=H_{\mathrm{eff}}{}^2(\mathrm{Tr}\mathcal{H}_d{}^{02}/\mathrm{Tr}\mathcal{H}_z{}^2) \tag{9}$$

and the quadrupolar contribution is given by

$$H_Q{}^2=H_{\mathrm{eff}}{}^2(\mathrm{Tr}\mathcal{H}_q{}^{02}/\mathrm{Tr}\mathcal{H}_z{}^2). \tag{10}$$

The requirement of rapid transfer of energy necessitates that $H_Q{}^2\lesssim H_D{}^2$ so that the trace over $\mathcal{H}_q{}^{02}$ in Eq. (10) includes only those Al spins with sufficiently small q. The square of the local field H_L is defined by

$$H_L{}^2=H_D{}^2+H_Q{}^2. \tag{11}$$

Relaxation in the rotating frame has been discussed by Redfield[9] and Solomon and Ezratty.[10] Assuming that at all times there is rapid transfer of energy between all parts of the spin system, $\langle\mathcal{H}_z\rangle$, $\langle\mathcal{H}_d{}^0\rangle$, and $\langle\mathcal{H}_q{}^0\rangle$, must satisfy Eq. (8) during relaxation to the lattice. We postulate elemental relaxation processes, however, which change $\langle M_z\rangle$, $\langle M_x\rangle$, $\langle\mathcal{H}_d{}^0\rangle$, and $\langle\mathcal{H}_q{}^0\rangle$ according to the equations

$$\partial\langle M_z\rangle/\partial t=(M_0-\langle M_z\rangle)/T_a, \tag{12a}$$

$$\partial\langle M_x\rangle/\partial t=-\langle M_x\rangle/T_b, \tag{12b}$$

$$\partial\langle\mathcal{H}_d{}^0\rangle/\partial t=(\langle\mathcal{H}_d{}^0\rangle_l-\langle\mathcal{H}_d{}^0\rangle)/T_D, \tag{12c}$$

and

$$\partial\langle\mathcal{H}_q{}^0\rangle/\partial t=(\langle\mathcal{H}_q{}^0\rangle_l-\langle\mathcal{H}_q{}^0\rangle)/T_Q, \tag{12d}$$

where

$$M_0=CH_0/\theta_l,\quad \langle\mathcal{H}_d{}^0\rangle_l=-CH_D{}^2/\theta_l,$$

and

$$\langle\mathcal{H}_q{}^0\rangle=-CH_Q{}^2/\theta_l.$$

Using Eqs. (8) and (12) and an alternative expression for the energy

$$\begin{aligned}E&=\langle\mathcal{H}_z\rangle+\langle\mathcal{H}_d{}^0\rangle+\langle\mathcal{H}_q{}^0\rangle\\&=-h_0\langle M_z\rangle-H_1\langle M_x\rangle+\langle\mathcal{H}_d{}^0\rangle+\langle\mathcal{H}_q{}^0\rangle,\end{aligned} \tag{13}$$

one can show that M the magnitude of the magnetization, relaxes towards the equilibrium value M_{eq} given by

$$M_{\mathrm{eq}}=\frac{M_0H_{\mathrm{eff}}(h_0/T_a+H_D{}^2/H_0T_D+H_Q{}^2/H_0T_Q)}{h_0{}^2/T_a+H_1{}^2/T_b+H_D{}^2/T_D+H_Q{}^2/T_Q} \tag{14}$$

with a time constant $T_{1\rho}$, given by

$$\frac{1}{T_{1\rho}}=\frac{1}{h_0{}^2+H_1{}^2+H_D{}^2+H_Q{}^2}\times\left\{\frac{h_0{}^2}{T_a}+\frac{H_1{}^2}{T_b}+\frac{H_D{}^2}{T_D}+\frac{H_Q{}^2}{T_Q}\right\}. \tag{15}$$

If we ignore terms of order H_D/H_0 and H_Q/H_0 in Eq. (14), then exactly at resonance $M_{\mathrm{eq}}=0$, and

$$\frac{1}{T_{1\rho}}=\frac{1}{H_1{}^2+H_D{}^2+H_Q{}^2}\left\{\frac{H_1{}^2}{T_b}+\frac{H_D{}^2}{T_D}+\frac{H_Q{}^2}{T_Q}\right\}. \tag{16}$$

We separate the electronic and diffusional contributions to each nuclear relaxation term on the right, and write $1/T_{1\rho}=(1/T_e)+(1/T_{\mathrm{diff}})$. The electronic contribution caused by the Fermi hyperfine contact interaction between the conduction electrons and the nuclear spins is given by[9–12]

$$\frac{1}{T_e}=\frac{1}{T_{1e}}\frac{H_1{}^2+\alpha H_D{}^2+\beta H_Q{}^2}{H_1{}^2+H_D{}^2+H_Q{}^2}, \tag{17}$$

[9] A. G. Redfield, IBM J. Res. Dev. **1**, 19 (1957).
[10] I. Solomon and J. Ezratty, Phys. Rev. **127**, 78 (1962).
[11] A. G. Anderson and A. G. Redfield, Phys. Rev. **116**, 583 (1959).
[12] L. C. Hebel, Jr., Phys. Rev. **128**, 21 (1962).

where α and β are constants approximately equal to 2 and 3, respectively. $1/T_{1e}$ is the high-field spin-lattice relaxation rate which is proportional to θ_l. The second contribution to nuclear relaxation is due to atomic diffusion. It will be examined in two limiting cases: that of rapid atomic motion or short motional correlation time, treated in part B of this section; and slow atomic motion or long correlation time, treated in part C of this section.

B. Diffusion Effects in the Rotating Frame—Rapid Motion

In the case of rapid atomic motion or weak collisions the local field interactions are treated as perturbations on the Zeeman interaction, and the relaxation theory of Bloembergen, Purcell, and Pound (BPP)[13] is applicable. This theory may be used as long as the average time between atomic jumps $\tau<T_{2\mathrm{RL}}$, where $T_{2\mathrm{RL}}$ is the rigid lattice spin-phase coherence time. For the dipolar interaction, the relaxation rate in the rotating frame due to the atomic motion is given by[14]

$$1/T_{D\,\mathrm{diff}}=3\gamma^2H_D^2(1-g)\tau_{\mathrm{Al}}/(1+4\omega_1^2\tau_{\mathrm{Al}}^2). \quad (18)$$

Here $\omega_1=\gamma H_1$, $(1-g)$ is a lattice sum of order unity that accounts for the fact that only part of the dipolar interaction is motion-dependent, and τ_{Al} is the average time between jumps for an aluminum atom.

The contribution to the relaxation rate due to the interaction of the Al^{27} nuclei with the rapidly fluctuating electric field gradients caused by the relative atomic motion of the solvent and solute atoms may be shown,[15] extending arguments of Abragam,[16] to be given by

$$1/T_{Q\,\mathrm{diff}}=3\gamma^2\tilde{H}_Q^2(1-g)\tau_c/(1+4\omega_1^2\tau_c^2). \quad (19)$$

Here $(1/\tau_c)=(1/\tau_{\mathrm{Al}})+(1/\tau_{\mathrm{imp}})$ and τ_{imp} is the mean time between impurity atom jumps. $\tilde{H}_Q^2$ is the mean-square quadrupole field evaluated over *all* Al sites, to be discussed further in Sec. IV.

C. Diffusion Effects in the Rotating Frame—Slow Motion

The dipolar interaction has been treated in detail by Slichter and Ailion[6] for the slow motion case ($\tau>T_{2\mathrm{RL}}$). They employ two assumptions: (1) The spin system couples together strongly enough to attain a common temperature between atomic jumps; (2) the actual time a nucleus spends in a jump, $\sim10^{-12}$ sec, is so short compared to a nuclear precession period that we can assume all spins have the same orientation just after a jump as they do just before a jump (sudden approximation). This strong collision theory of atomic diffusion leads to

$$1/T_{D\,\mathrm{diff}}=2(1-p)/\tau_{\mathrm{Al}}. \quad (20)$$

Here $(1-p)$ is a lattice sum of order unity that accounts for the fact that the local field at a nucleus after a jump is not statistically independent of the local field before the jump.

Although Eqs. (18) and (20) as written exhibit only the solvent jump time τ_{Al}, the dipolar relaxation will in general involve both the solute and solvent jump times in alloys. It happens that the solutes of interest in the present study make a negligible contribution to the dipolar energy and the dipolar relaxation rate because of their small nuclear dipole moments and low abundance. Equations (18) and (20) are thus rigorously applicable to pure Al, and are excellent approximations in the alloys to be considered. Of course τ_{Al} in an alloy may itself depend upon the solute species and concentration.

To consider the motional contribution to nuclear relaxation by the quadrupolar interaction, we use the Hamiltonian in Eq. (6) and assume for simplicity that for a dilute random distribution of solutes q_{ik} is simply proportional to R_{ik}^{-3}, where R_{ik} is the distance between the kth solute and the ith aluminum nucleus. In any atomic jump, the quadrupolar Hamiltonian changes, since the relative coordinates of the solutes and the Al^{27} nuclei change. Letting $\mathcal{H}_q^0$ be the quadrupolar Hamiltonian before the jump and $\mathcal{H}_{qf}^0$ be the quadrupole Hamiltonian after the jump, the change in energy in an atomic jump is given by

$$\Delta E_q=[1/k\theta(2I+1)N_{\mathrm{Al}}]\,\mathrm{Tr}[(\mathcal{H}_q^0)^2-\mathcal{H}_q^0\mathcal{H}_{qf}^0]. \quad (21)$$

In arriving at Eq. (21) we have employed the sudden approximation according to which the density matrix is the same before and immediately after a jump; N_{Al} is the number of Al nuclei in spin-temperature equilibrium.

The expectation value of the quadrupole energy is

$$\langle\mathcal{H}_q^0\rangle=-U\sum_{i,k}B_{ik}^2=-\frac{CH_Q^2}{\theta}, \quad (22)$$

where U contains constants and traces over spin variables, and $B_{ik}=(1-3\cos^2\phi_{ik})/R_{ik}^3$, with i indicating solvent positions and k indicating solute positions. In the sum over i in Eq. (22) and for the sums which appear in the remainder of this section, the use of a common spin temperature leads to the restriction on i that B_{ik}^2 may take only values less than some maximum such that $H_Q^2\lesssim H_D^2$. The same reasons apply here as were given following Eq. (10); they are discussed further in Sec. IV.

Assuming a random distribution of solute atoms in dilute solution we may approximate Eq. (22) in the

[13] N. Bloembergen, E. M. Purcell, and R. V. Pound, Phys. Rev. 73, 679 (1948).
[14] D. C. Douglas and G. P. Jones, J. Chem. Phys. 45, 956 (1966).
[15] F. Y. Fradin, thesis, University of Illinois, 1967 (unpublished).
[16] A. Abragam, *The Principles of Nuclear Magnetism* (Oxford University Press, London, 1961).

forms

$$-\langle \mathcal{H}_q^0\rangle \cong UN_{\text{imp}}\sum_i B_{ik}^2 \cong UN_{\text{imp}}\frac{N_{\text{Al}}}{N}\sum_\alpha{}' B_{\alpha k}^2, \quad (23)$$

where the summation over α includes all lattice sites (except the solute site k) and the prime indicates that the terms $B_{\alpha k}^2$ of the sum are subject to the restriction mentioned in the previous paragraph. In practice this amounts to omitting the $B_{\alpha k}^2$ of two or three shells of solvents near the solute. In Eq. (23), N_{imp} is the number of impurities, N_{Al} is the number of aluminum nuclei in spin-temperature equilibrium, and N is the total number of sites included in the sum.

Equations (21) and (23) are the basic relations needed to construct an expression of the form of Eq. (12d) for the time dependence of the quadrupolar energy. A crucial characteristic of the model we propose is that the vacancies themselves move so rapidly that the effects of their electric gradients are negligible. This point of view is strengthened by the belief that motional quadrupolar effects play no part in the relaxation of pure Al up to the melting point. Our detailed analysis thus proceeds as if the condition $\tau_v > T_{2\text{RL}}$, required for spin-temperature equilibrium, prevails, whereas it is equally important to remember that $\delta\omega_{Qv}\tau_v \ll 1$ must apply in order to average out vacancy effects. Here $\delta\omega_{Qv}$ is the quadrupole splitting caused by the vacancy at rest. The condition $\tau_{\text{imp}}, \tau_{\text{Al}} > T_{2\text{RL}}$ remains satisfied since, considering all jumps, $[(N_{\text{Al}}/\tau_{\text{Al}})+(N_{\text{imp}}/\tau_{\text{imp}})]=N_v/\tau_v$, and $N_{\text{Al}}, N_{\text{imp}} \gg N_v$. We conceive of a vacancy jumping into a region of lattice and diffusing through it, leaving a trail of displaced solvent and solute atoms. These nuclei, as well as others not displaced by this encounter, now relax toward the equilibrium temperature of the spin system. Equilibrium in the new local field will be achieved before these solvent and solute atoms jump again in the mean. We attempt to diminish the discrepancy between the model we treat and the physically more realistic one for which $\tau_v < T_{2\text{RL}}$ by introducing a numerical factor, less than unity, to account for this correlation of fields. The quadrupole problem is, in this regard, formally less severe than the dipolar case of SA because our solvent nuclei are not coupled to each other by electric effects; however, dipolar fields are a large fraction of the local field in our case also.

We wish to derive the change in average energy involved in each solute and solvent jump. Using the respective jump rates we then relate these changes to $T_{Q\,\text{diff}}$. When any atom jumps, we have, from Eq. (21),

$$\Delta E_q = U\sum_{i,k}(B_{ik}^2 - B_{ik}B_{ik}^{(q)}), \quad (24)$$

where $B_{ik}^{(q)}$ is the value of B_{ik} after the jump. For all atoms that do not jump $B_{ik}^{(q)}=B_{ik}$. For the jump of the nth solute into the pth vacancy

$$\Delta E_{\text{imp}} = U\sum_i(B_{in}^2 - B_{in}B_{ip}); \quad (25)$$

all solvents move relative to the nth solute. Because we are considering alloys which are dilute and random, a sum over i for a given k is proportional to a sum over all sites, so that

$$\Delta E_{\text{imp}} \approx U\frac{N_{\text{Al}}}{N}\sum_\alpha{}'(B_{\alpha n}^2 - B_{\alpha n}B_{\alpha p}) \quad (25')$$

and using a lattice sum defined by

$$p' = \sum_\alpha{}' B_{\alpha n}B_{\alpha p}/\sum_\alpha{}' B_{\alpha n}^2,$$

we can write

$$\Delta E_{\text{imp}} = U\frac{N_{\text{Al}}}{N}(1-p')\sum_\alpha{}' B_{\alpha n}^2 = -\frac{1}{N_{\text{imp}}}(1-p')\langle \mathcal{H}_q^0\rangle. \quad (26)$$

Equation (23) was used, and the impurities assumed to be sufficiently separated that (26) represents the energy change for any impurity jump, i.e., it is an average impurity jump energy.

For the jump of the rth Al atom into the qth vacancy, from (24),

$$\Delta E_{\text{Al}} = U\sum_k(B_{rk}^2 - B_{rk}B_{qk}) \quad (27)$$

is the expectation value of the change in energy for the Al nucleus originally at site r. This must be averaged over all possible Al jumps, from any site α to any neighboring site α'. Thus the average energy for a single Al atom jump is

$$\langle \Delta E_{\text{Al}}\rangle_{\text{av}} = \frac{U}{NG}\sum_\alpha{}^N{}'\sum_{\alpha'}{}^G\sum_k(B_{\alpha k}^2 - B_{\alpha k}B_{\alpha' k}), \quad (28)$$

which can be approximated

$$\langle \Delta E_{\text{Al}}\rangle_{\text{av}} = \frac{UN_{\text{imp}}}{NG}(1-p'')\sum_\alpha{}' B_{\alpha k}^2 = -\frac{1}{N_{\text{Al}}}(1-p'')\langle \mathcal{H}_q^0\rangle, \quad (29)$$

upon introducing

$$p'' = \frac{1}{G}\sum_\alpha{}'\sum_{\alpha'}{}^G B_{\alpha k}B_{\alpha' k}/\sum_\alpha{}' B_{\alpha k}^2,$$

and using Eq. (23) as before. G, the number of possible jumps for an Al atom is equal to the number of near-neighbor sites; the order of the α and k summations can be reversed because of the statistical independence of the solute and solvent positions on the lattice. It can be seen that $p''=p'$ if we neglect the effect of the vacancy on the field gradient.

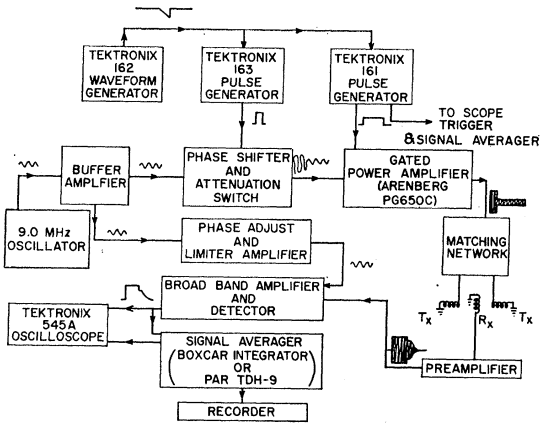

FIG. 1. Block diagram of the pulse apparatus. The cross-coil configuration is used so that the transmitter coil, receiver coil, and static field direction are mutually orthogonal.

The total rate of change of the quadrupole energy caused by atomic diffusion is the sum of the above contributions;

$$\partial\langle\mathcal{H}_Q^0\rangle/\partial t=(N_{\rm imp}/\tau_{\rm imp})\Delta E_{\rm imp}+(N_{\rm Al}/\tau_{\rm Al})\langle\Delta E_{\rm Al}\rangle_{\rm av}. \quad (30)$$

Equation (30) predicts that the spin temperature will approach infinity ($\langle\mathcal{H}_Q^0\rangle\rightarrow 0$) whereas taking proper account of the lattice leads to the correct result that the spin temperature relaxes to the lattice temperature; accordingly, we rewrite Eq. (30):

$$\partial\langle\mathcal{H}_Q^0\rangle/\partial t=(\langle\mathcal{H}_Q^0\rangle_l-\langle\mathcal{H}_Q^0\rangle)(1-p')\times(1/\tau_{\rm imp}+1/\tau_{\rm Al}). \quad (30')$$

Comparison with Eq. (12d) shows that

$$1/T_{Q\,\rm diff}=(1-p')(1/\tau_{\rm imp}+1/\tau_{\rm Al}). \quad (31)$$

Thus, in the low-temperature slow-atomic-motion region the total relaxation rate from Eqs. (16), (17), (20), and (31), (including electronic and motional contributions) is found to be

$$\frac{1}{T_{1\rho}}=\frac{1}{T_{1e}}\cdot\frac{H_1^2+\alpha H_D^2+\beta H_Q^2}{H_1^2+H_D^2+H_Q^2}+\frac{1}{H_1^2+H_D^2+H_Q^2}\times\left[2H_D^2(1-p)\frac{1}{\tau_{\rm Al}}+H_Q^2(1-p')\left(\frac{1}{\tau_{\rm Al}}+\frac{1}{\tau_{\rm imp}}\right)\right]. \quad (32)$$

III. EXPERIMENTAL

A. Techniques

In order to measure the magnetization in the rotating frame, the "spin-locking" sequence[17] was employed. This technique consists of applying an intense rf pulse at the resonant frequency to tip the equilibrium magnetization into the plane normal to H_0 in a time $t_{\pi/2}$, short compared with $T_{2\rm RL}$. This is immediately followed by an rf magnetic field H_1 of amplitude comparable to the local field H_L. H_1 is also at the resonant frequency but is phase shifted 90° relative to the initial pulse. Thus, in a time of the order of $T_{2\rm RL}$, the effective field has been reduced from a value large compared with H_L to a value comparable to H_L. In addition, the direction of the magnetization is changed from alignment parallel to H_0 to alignment parallel to H_1. After a time t the rf field H_1 is abruptly turned off and the height of the free induction decay (FID) is measured. The cycle is repeated, but H_1 is allowed to remain on for a longer period of time. The decrease in amplitude of the FID for different pulse lengths is thus a measure of the relaxation of the total magnetization in the presence of H_1.

All measurements were done exactly at resonance. Since $M_{\rm eq}\approx 0$ at the center of the line, the center of the resonance line was determined by adjusting the magnetic field so that a null in the signal is observed for pulse lengths long compared to T_1. The rf field H_1 was calibrated using successive 180° pulses to give consecutive nulls in the FID.

B. Apparatus

A block diagram of the apparatus used in this experiment is shown in Fig. 1. It is a crossed-coil pulse rig, consisting of a transmitter, broad-band receiver, and signal-averaging equipment. The transmitter consists of a continuous-wave 9.0-MHz crystal oscillator and a gated amplifier capable of generating successive pulses which differ in both rf phase and amplitude. A maximum H_1 of about 15 G was used in these experiments.

The receiver coil is connected to a preamplifier consisting of two cascode stages. The signal from the preamplifier as well as a 9.0-MHz reference signal from the oscillator is fed into a four-stage broad-band tuned amplifier followed by a diode detector. The use of a reference voltage which is larger than the signal assures that the diode detector will at all times be biased into the linear region. For this reason noise never contributes to the dc output level even when the signal is smaller than the noise. The bandwidth of the receiver is about 600 kHz.

In order to improve the signal-to-noise ratio, signal-averaging methods were employed. In the early work a double-boxcar integrator similar to that employed by Holcomb and Norberg[4] was used. In the latter part of the work, a Princeton Applied Research Waveform Eductor was used as a synchronous integrator.

The high-temperature probe is capable of operating to 700°C. A Lava coil form for the platinum wire transmitter coil fits into a Lava tube that is noninductively wound with a nichrome wire heater coil. The heater coil is driven by a dc power supply that is steplessly controlled by a thermocouple actuated temperature

[17] S. R. Hartmann and E. L. Hahn, Phys. Rev. 128, 2042 (1962).

controller. The probe assembly is mounted in a water-cooled brass container that fits into the 3-in. gap of a Harvey-Wells 12-in. electromagnet. Using this probe it was always possible to hold the temperature of the sample constant to within ± 0.5°C. The temperature of the sample was determined by means of a Pt-Pt+10% Rh thermocouple placed in contact with the sample capsule.

C. Alloy Preparation

The aluminum-based alloys used in this investigation were prepared from 99.999% pure Al and high-purity Zn, Mg, and Ag. The alloys were prepared in approximately 20-g ingots. Melting was carried out in an induction furnace under an argon atmosphere using spectroscopic purity graphite crucibles. The alloys were subsequently heavily swaged and annealed below their solidus temperature to promote homogenization.

A center section of each ingot was filed to produce powder which passed through a 325-mesh seive (44μ openings). The classical skin depth for 9-MHz radiation at room temperature is 30 μ for pure Al. To prevent sintering of the metal powders at high temperature the particles were dispersed in thorium oxide and sealed in quartz capsules.

IV. EXPERIMENTAL RESULTS AND DISCUSSION

A. H_1 Dependence of the Initial Magnetization

In the spin-locking pulse sequence described in Sec. IIIA, the Hamiltonian is independent of time for $t_{\pi/2}<t \ll T_{1\rho}$. Therefore, we may determine the H_1 dependence of the initial magnetization ($t \ll T_{1\rho}$) in the rotating frame by equating the energy given by Eq. (8) to the energy immediately after the $\frac{1}{2}\pi$ pulse $E(t_{\pi/2}{}^+)$. Using the sudden approximation that $\rho(t_{\pi/2}{}^+)=\rho(t_{\pi/2})$ we find[15]

$$M=M_0[H_1{}^2/(H_1{}^2+H_D{}^2+H_Q{}^2)]. \tag{33}$$

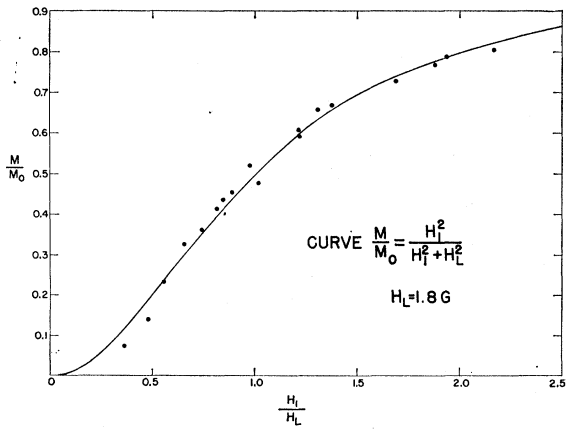

FIG. 2. Dependence of the initial nuclear magnetization of pure Al on the spin-locking field amplitude H_1. Data obtained using phase incoherent detection at 23°C.

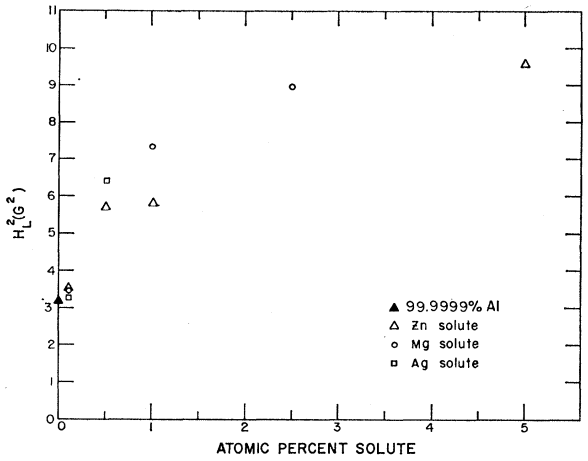

FIG. 3. $H_L{}^2$ as a function of solute concentration at 23°C. $H_L{}^2$ is determined from the dependence of the initial magnetization on the amplitude of the spin-locking field H_1.

Figure 2 exhibits the results of measurements of the initial magnetization for various amplitudes of the rf field H_1 at room temperature in nominally 99.9999% pure Al. A good fit to the data is obtained using Eq. (33) as shown by the solid line. If we take $H_Q{}^2=0$ in pure Al, $H_D{}^2$ is found to be equal to 3.2 G^2. Since the van Vleck second moment of the resonance absorption line for a powder is given by[18] $\langle \Delta H_D{}^2 \rangle = 3H_D{}^2$, we find $\langle \Delta H_D{}^2 \rangle = 9.6 \pm 0.9$ G^2. This confirms the high values found in many other experiments on Al[5] as compared with the theoretical value of 7.63 G^2. The discrepancy between the theoretical and experimental value is still unexplained.

The values of $H_L{}^2=H_D{}^2+H_Q{}^2$ determined from the dependence of the initial magnetization on H_1 are presented in Fig. 3 as a function of composition for all the alloys studied. It can readily be shown that $H_Q{}^2 = \frac{1}{3}\langle \Delta H_Q{}^2 \rangle$, where $\langle \Delta H_Q{}^2 \rangle$ is the quadrupolar contribution to the second moment of the absorption line for a powder, given by[19]

$$\langle \Delta H_Q{}^2 \rangle = \frac{9}{400}\left(\frac{e^2Q}{\gamma\hbar}\right)\frac{(2I+3)}{I^2(2I-1)}\frac{1}{N}\sum_i^N q_i{}^2. \tag{34}$$

If from $H_L{}^2$ we subtract $H_D{}^2$, which is independent of alloying for the solutes and concentrations of interest in this work, and then make use of Eq. (34), we may determine an experimental value of the average squared electric field gradient $\langle q^2 \rangle_{\rm av} = (1/N)\sum_i{}^N q_i{}^2$ at an aluminum nucleus that is in spin-temperature equilibrium.

Under the conditions of spin-temperature equilibrium implicit in the use of Eqs. (33) and (34) in the slow-motion (low-temperature) region, the value of $\langle q^2 \rangle_{\rm av}$ includes contributions from only those Al nuclei which lie at sites where the magnitude of the electric-

[18] L. C. Hebel, in *Solid State Physics*, edited by F. Seitz and D. Turnbull (Academic Press Inc., New York, 1963), Vol. 15.
[19] L. S. Brown, IBM J. Res. Dev. **6**, 338 (1962).

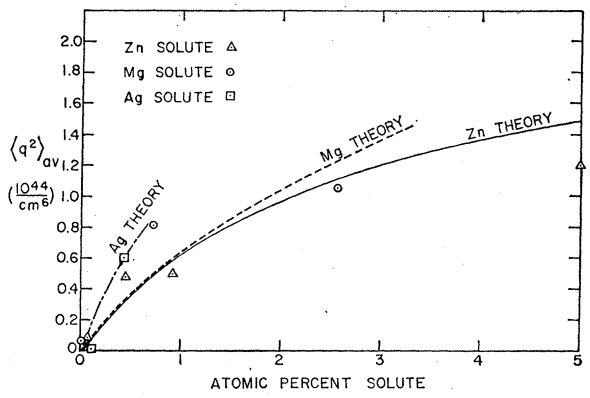

FIG. 4. Theoretical and experimental values of $\langle q^2\rangle_{av}$ for Zn, Mg, and Ag solutes in Al. The experimental points are obtained from H_L^2 measured at 23°C.

field gradient is less than some critical value q_c. An Al spin which is exposed to a gradient greater than q_c would have a quadrupole interaction energy much greater than the dipolar interaction energy and would not come into spin-temperature equilibrium with the rest of the spin system in times short compared to $T_{1\rho}$. The value of $\langle q^2\rangle_{av}$ derived from experiment via Eq. (34) is thus to be compared with the theoretical value derived using a suitably truncated summation omitting terms for which $|q_{ik}|>q_c$.

Blandin and Friedel have calculated the spatial dependence of the electric field gradient about a solute i due to conduction-electron screening in Al.[20] This is given for large distances R_{ik} by

$$q_{ik}=q(R_{ik})=A[\cos(2k_FR_{ik}+\phi)/R_{ik}^3], \qquad (35)$$

where $A=(4/3\pi)\alpha\mu$. Here α and ϕ depend on the phase shifts of the scattered partial waves and are calculated assuming that only the η_0 and η_1 phase shifts are nonzero. μ is a constant enhancement factor for a given host and is taken to be 15 for Al. η_0 and η_1 are calculated from a modified Friedel sum rule[21]

$$Z_{\text{eff}}=-\frac{2}{\pi}\sum_l(2l+1)\eta_l(k_F) \qquad (36)$$

and the additional resistivity due to impurities in a metal given by[22]

$$\Delta\rho=\frac{2hc}{Ze^2k_F}\sum_{l=1} l\sin^2[\eta_{l-1}(k_F)-\eta_l(k_F)], \qquad (37)$$

where c is the atomic fraction of solute, Z is the valence of the host, k_F is the magnitude of the Fermi wave vector of the host, e is the charge of an electron, h is Planck's constant, l is the angular-momentum quantum number of the scattered partial wave, and Z_{eff} is the effective valence difference between the solute and solvent.

The parameters we used to calculate $q(R_{ik})$ are presented in Table I for Al as solvent. The values for Zn and Mg solutes were calculated by Blandin and Friedel[20] using Vassels'[23] resistivity data. The values for the silver solute were calculated using Robinson and Dorn's[24] resistivity data.

In calculating $\langle q^2\rangle_{av}$ we make two simplifying assumptions: (a) The gradient at a site equidistant from two or more solute atoms is equal to that due to one solute at that distance. (b) All contributions to q_{ik} other than the largest are ignored. Consider first a mean-square gradient at a solvent atom computed for a random solid solution with no limitation on the magnitude of q_{ik}. Let $q_{ik}=q_s$, where s designates the shell at $|R_{ik}|$. Then

$$\langle q^2\rangle_{\text{all}}=\sum_s P_sq_s^2, \qquad (38)$$

with $P_s=(1-c)^{N_s}[1-(1-c)^{n_s}]$, and $N_s=\sum_i^{(s-1)} n_i$; P_s is the probability of there being no solute atoms in shells $1,\cdots,(s-1)$ around an Al atom, and one or more solutes in the sth shell. n_s is the number of sites in the sth shell, and $\sum P_s=1$. $\langle q^2\rangle_{\text{all}}$ is used in Eq. (34) to define $\tilde{H}_Q^2$, the untruncated mean-square quadrupole field needed in the high-temperature region; see Eq. (19). For the low-temperature region it is necessary to obtain a theoretical $\langle q^2\rangle_{av}$ for only those Al nuclei in spin-temperature equilibrium; accordingly we modify N_s to include the requirement that no solute atoms occupy sites in shells at which $|q_s|>q_c$. Also terms for which $|q_s|>q_c$ must be deleted from the sums. With these two changes we arrive at the desired $\langle q^2\rangle_{av}$ for comparison with experiment, namely,

$$\langle q^2\rangle_{av}=\sum_s{}' P_s'q_s^2, \qquad (39)$$

where

$$P_s'=(1-c)^{N_s'}[1-(1-c)^{n_s}],$$

$$N_s'=\sum_i^{(s-1)}{}' n_i,$$

and

$$\sum_s{}' P_s'=1.$$

The prime on the summations indicates that the sums

TABLE I. Calculated phase shifts in aluminum.

Solute	Z_{eff}	$\Delta\rho(\mu\Omega$ cm/at.%)	η_0	η_1	α	ϕ
Zn	−0.9	0.35	−0.715	−0.228	0.32	2.11
Mg	−1.68	0.60	−2.403	−0.078	0.51	2.12
Ag	−2.00	1.13	−1.250	−0.630	1.136	−0.124

[20] A. Blandin and J. Friedel, J. Phys. Radium **21**, 689 (1960); T. J. Rowland, Acta Met. **3**, 74 (1955).
[21] F. J. Blatt, Phys. Rev. **108**, 285 (1957).
[22] K. Huang, Proc. Phys. Soc. **60**, 161 (1948).
[23] C. R. Vassels, J. Phys. Chem. Solids **7**, 90 (1958).
[24] A. T. Robinson and J. E. Dorn, J. Metals **3**, 457 (1951).

do not include terms for shells with $|q_s|>q_c$.[25] The sums in Eqs. (38) and (39) were evaluated to the 47th shell with $q_s=q(R_{ik})$ from Eq. (35), $\mu=15$,[20] and the cutoff gradient, $q_c=1.7\times10^{22}$ cm^{-3}. The curves in Fig. 4 show the calculated $\langle q^2\rangle_{av}$ as a function of solute concentration. Gradients greater than 1.7×10^{22} cm^{-3} at a nucleus appear to effectively inhibit its contact with the equilibrium spin system. This value of q_c was found to be the best choice, within about $\pm10\%$, for all three solutes, Zn, Mg, and Ag. The consistancy does not depend critically upon the values derived from Eq. (35), it confirms the form of Eq. (35), and the concept that certain Al spins are not in contact with the spin system because of large electric-field gradients, independently of the solute species. The above value for q_c is also consistent with Fernelius'[26] estimate of the largest gradient contributing to the width of the nonresonant spin absorption ($q_{max}\approx2\times10^{22}$ cm^{-3}) in dilute Al-Zn alloys.

B. Temperature Dependence of $T_{1\rho}$

In a previous paper by the authors,[27] it was shown that in pure Al, $1/T_{diff}$ could be entirely accounted for by the dipolar interaction. From the activation energy for diffusion derived from $1/T_{diff}$ and a value of 0.76 eV for the formation energy of a vacancy in pure Al,[28] a value of 0.49 eV was determined for the energy of single-vacancy migration in pure Al.

In both the high-temperature, rapid motion region, and the low-temperature, slow motion region, $1/T_{1\rho}$ has one contribution arising from atomic diffusion and another from the hyperfine interaction of the nucleus with the conduction electrons. Since it is a transition probability these contributions add [see below Eq. (16)] so that,

$$1/T_{1\rho}=1/T_e+1/T_{diff}. \tag{40}$$

The electronic contribution $1/T_e$ is given in the low-temperature region by Eq. (17); in the high-temperature region where BPP theory applies $1/T_e=1/T_{1e}$. The diffusion contribution is given in the low-temperature region by [cf. Eq. (32)],

$$1/T_{diff}=[1/(H_1^2+H_L^2)][2(1-p)H_D^2(1/\tau_{Al})+(1-p')H_Q^2(1/\tau_{Al}+1/\tau_{imp})], \tag{41}$$

and in the high-temperature region ($2\omega_1\tau_c\ll1$) by

$$1/T_{diff}=3\gamma^2H_D^2(1-g)\tau_{Al}+3\gamma^2\tilde{H}_Q^2(1-g)\tau_c. \tag{42}$$

The quantities appearing in these equations have all been defined previously. Since τ_{Al} and τ_{imp} are exponentially dependent on reciprocal temperature, whereas $1/T_{1e}$ is directly proportional to temperature, we subtract the electronic contribution to $1/T_{1\rho}$ to obtain $1/T_{diff}$. The values of $\log(1/T)_{diff}$ for four alloys of Zn in Al are shown in Fig. 5 as a function of reciprocal temperature. It is apparent from the aspect of the data plotted in this way that within certain temperature intervals we are dealing with a functional dependence of the form $(1/T)_{diff}\propto e^{\pm Q/RT}$ ordinarily encountered in activated processes. A first impulse may be to view Q as the activation energy for diffusion of the species under observation, Al in the present instance. We believe this approach to be incorrect, as the foregoing analysis should testify. Figures 6 and 7 display the $\log(1/T)_{diff}$ versus $1/\theta$ data for Al^{27} with Ag and Mg, respectively, present as solute.

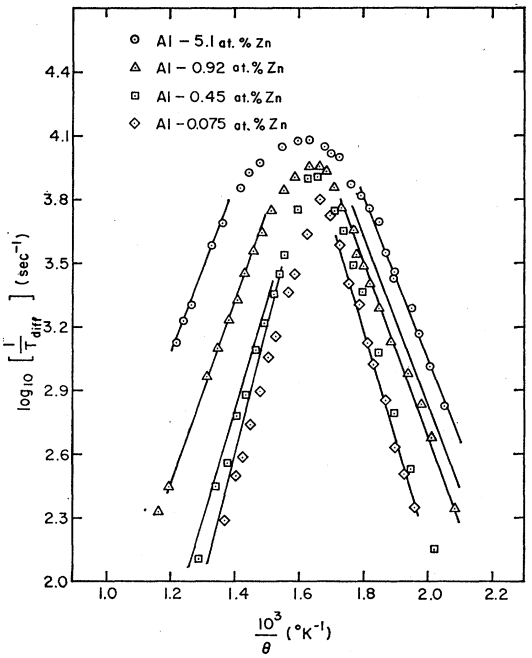

FIG. 5. Temperature dependence of the diffusion contribution to $T_{1\rho}$ for Al-Zn alloys. The solid lines are the calculated values as explained in the text.

The salient features of the data presented in Figs. 5–7 are (a) the marked increase in relaxation rate (at a given temperature) with solute concentration; (b) the decrease in the magnitude of the slope of the straight line portions as the solute concentration is increased, (c) the equality, within the accuracy of our measurements, of the low- and high-temperature slopes (with opposite signs) for a given concentration, (d) the *different* relative increase in $1/T_{diff}$, for a given concentration, in the high- and low-temperature regions, (e) the striking differences in the over-all behavior of the curves for different solutes (compare Zn or Ag with Mg).

To interpret these experimental results we use a rather simplified model based on a first-order vacancy-

[25] These are, for Zn, $s=1, 2$; for Mg, $s=1, 2, 3$; for Ag, $s=1, 4, 5$.
[26] N. Fernelius, thesis, University of Illinois, 1966 (unpublished).
[27] F. Y. Fradin and T. J. Rowland, Appl. Phys. Letters **11**, 207 (1967).
[28] R. Simmons and R. Balluffi, Phys. Rev. **117**, 52 (1960).

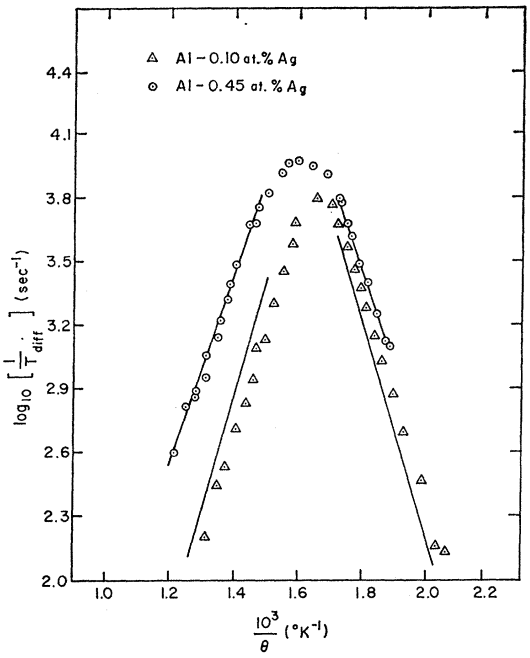

FIG. 6. Temperature dependence of $1/T_{\text{diff}}$ for dilute Al-Ag alloys. The relaxation rate increases rapidly with concentration in the high-temperature region. The solid lines are calculated values.

impurity binding mechanism. For the impurity jump rate we use

$$1/\tau_{\text{imp}}=12K_2w_2e^{-(E_f-B_{iv})/k\theta}, \tag{43}$$

where B_{iv} is the vacancy-impurity binding energy, E_f is the formation energy of a vacancy in Al, w_2 is the probability per second that an impurity atom jumps into a vacant nearest-neighbor sites, and K_2 is an entropy factor associated with vacancy-impurity pair formation. The probability of one vacancy occurring among the nearest-neighbor sites is just $12\exp[-(E_f-B_{iv})/k\theta]$.

The reader familiar with the literature of microscopic diffusion processes may question our use of w_2 rather than some weighted average of the jump frequencies which ultimately determine the progress of the solute through the lattice. Such an average enters importantly into any similar discussion of chemical or tracer diffusion through the correlation factor f.[1] The latter describes the effect of spatial correlation on atomic migration in terms of the various types of solute and solvent jumps involved. It is here that an essential difference between the resonance and tracer measurements becomes obvious, and the distinctive contribution of the resonance measurement is to be found. We are primarily concerned with temporal correlation, and our designation of τ_{imp} as the relevant correlation time assumes that no complex, many rapid jump, correlated process is causing an apparent impurity jump time, but that in fact we have single impurity jumps separated by a mean time τ_{imp}. Indeed if faster, multiple jump processes are taking place the jump times would be much less than $T_{2\text{RL}}$ in the low-temperature region, since τ_{imp} as we define it is approaching $T_{2\text{RL}}$ closely and is shorter than τ_{Al}. The point being emphasized here is that we are not simply measuring the solute self-diffusion coefficient D_2 in a different way. Remarks further comparing our results with those obtained by other techniques will be made below.

In the low-temperature region we set the aluminum jump rate

$$[1/\tau_{\text{Al}}(c)]=12K_0w_0e^{-E_f/k\theta}(1-12c)$$
$$=[1/\tau_{\text{Al}}(0)](1-12c), \tag{44}$$

where $w_0=\nu_0e^{-E_{m0}/k\theta}$ is the probability per second that an Al atom with no neighboring impurities jumps into a free vacancy at a nearest-neighbor site, and K_0 is the associated entropy factor for vacancy formation. τ_{Al} applies to the Al nuclei at the third-neighbor distance from an impurity and beyond, and should be properly applicable to the process to which $\langle\Delta E_{\text{Al}}\rangle_{\text{av}}$ [Eq. (29)] is appropriate. Al atoms nearer to solutes are not in spin-temperature equilibrium.

In the high-temperature region it was found that the best agreement was attained when τ_c was set equal to τ_{imp} for Zn and Ag. For Mg

$$[1/\tau_{\text{Al}}(c)]=[1/\tau_{\text{Al}}(0)]$$
$$\times\{1-12c+4c\exp[(E_{m0}-E_{m1}+B_{iv})/k\theta]\} \tag{44'}$$

was used in the expression for τ_c. The third term on the right in Eq. (44′) includes the effect of associated Al jumps, i.e., the type in which an Al atom next to an impurity jumps into a bound vacancy. The frequency of such an event, given the bound vacancy, is taken to be $w_1=\nu_1\exp(-E_{m1}/k\theta)$ and we assume $\nu_1=\nu_0$. The motion of Al nuclei near the impurity is important in the high-temperature region, since in that region the near nuclei are not excluded from the averaging, and $\tilde{H}_Q^2$ is used.

Equations (41)-(44′) were used as described to calculate curves of $1/T_{\text{diff}}$ versus $1/\theta$ by substituting trial values for the unknown parameters $(K_2\nu_2)$ and E_{m2}, where we have let $w_2=\nu_2\exp(-E_{m2}/k\theta)$. These curves were compared visually with the measured $1/T_{\text{diff}}$ results, and $K_2\nu_2$ and E_{m2} adjusted for a best fit. For $w_0=\nu_0\exp(-E_{m0}/k\theta)$, the values $\nu_0K_0=1/12\tau_0=1/(48\times10^{-15})$ sec^{-1} and $E_{m0}=0.49$ eV, published previously,[27] were used. The theoretical values of H_Q^2

TABLE II. Diffusion parameters.

Solute	B_{iv}(eV)[a]	E_{m2}(eV)[b]	$K_2\nu_2$ (sec^{-1})
Zn	0.19	0.21	1.5×10^{10}
Mg	0.18	0.28	5.0×10^{10}
Ag	0.08	0.15	2.0×10^{10}

[a] J. Takamura, in *Lattice Defects in Quenched Metals*, edited by R. M. J. Cotterill *et al.* (Academic Press Inc., New York, 1965).
[b] For Mg the value 0.37 eV was used for E_{m1} in Eq. (44′).

and $\tilde{H}_Q^2$ were derived from Eqs. (38), (39), and (34) as described in Sec. IVA; and values of $(1-p')=0.66$, 0.50, and 0.64 were used for Zn, Mg, and Ag, respectively. $(1-p)$ is 0.850 for Al, and $(1-g)=0.922$. The results of calculations in which the diffusion parameters listed in Table II were used are compared with the data in Figs. 5, 6, and 7. The values of B_{iv} in Table II are representative of those found in the literature, but are viewed as being very uncertain. Also we wish to emphasize that the values of E_{m2} listed in Table II should be considered to be estimates only, firstly because of the simplified model used to obtain them and secondly because of the uncertainty of the values of B_{iv} used to obtain them through Eq. (43). Table III compares the experimental and calculated slopes of the semilogarithmic plots of $1/T_{\text{diff}}$ versus $1/\theta$ for the alloys investigated.

It remains to compare the present results with mass-diffusion experiments in the case of the Al-Zn system. Our results indicate a rapid solute jump rate, while tracer measurements[29] of the diffusion of Zn into Al show D_{Zn}^* to be very nearly equal to $D_{\text{Al}}(0)$, the diffusion coefficient of pure Al. As we now show, these observations are consistent, and imply a rapid dependence of the correlation factor f on temperature. Again, we used the first-order impurity-vacancy binding model, according to which the correlation factor for the diffusion of the solute is given by[1]

$$f=W/(W+w_2), \tag{45}$$

where $W=w_1+\frac{7}{2}Fw_3$, w_3 is the dissociative jump frequency, F is a function of w_4/w_0, and w_4 is the associative jump frequency. w_1, w_2, and w_0 have been defined previously. Using standard expressions for D_{Zn}^* and D_{Al}, together with Eq. (45), Lidiard[30] showed that it was possible to express f in the alternative form

$$f=1-f_0\frac{w_0}{W}e^{-B_{iv}/k\theta}\frac{D_{\text{Zn}}^*}{D_{\text{Al}}(0)}, \tag{46}$$

TABLE III. Comparison of observed and calculated values of the slopes of the curves in Figs. 5–7 in the high- and low-temperature regions.[a]

Alloy	Q_{expt}(k cal/mole)	Q_{calc}(k cal/mole)
0.075 Zn	$24.7_5\pm0.5$	25.9 ± 1.8
0.45 Zn	24.6 ± 0.7	21.9 ± 1.9
0.92 Zn	18.4 ± 0.6	19.4 ± 0.2
5.11 Zn	17.9 ± 0.6	18.1 ± 0.1
0.10 Ag	$23.0_5\pm0.6$	24.7 ± 0.4
0.45 Ag	21.1 ± 0.7	20.7 ± 0.5
0.10 Mg	$27.7_5\pm1.0$	$27.6_5\pm1.0$
0.72 Mg	$24.2_5\pm0.6$	22.1 ± 1.0
2.56 Mg	21.1 ± 0.4	20.8 ± 0.7

[a] The deviations indicate either the standard deviation from a single exponential, or half the difference between the high- and low-temperature slopes, whichever is larger.

[29] Norman L. Peterson and Steven J. Rothman (to be published); Bull. Am. Phys. Soc. **12**, 324 (1967).

[30] A. B. Lidiard, Phil. Mag. **5**, 1171 (1960).

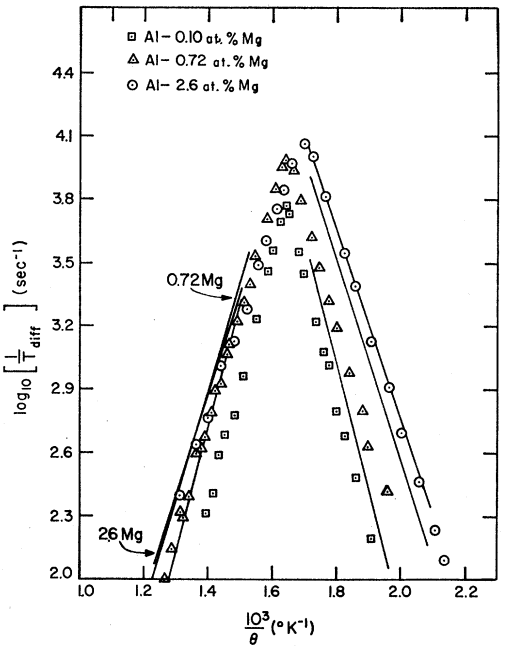

FIG. 7. Temperature dependence of the diffusion contribution to the relaxation rate in Al-Mg alloys. Contrast the high-temperature behavior with that of Al-Ag or Al-Zn. The solid lines are calculated values.

where w_2 enters only implicitly through D_{Zn}^*, for which Rothman and Peterson[31] find $0.256\exp(-28\,850/k\theta)$ cm^2/sec. Here, f_0 is the correlation factor for pure Al. Eliminating f between Eqs. (45) and (46) we solve for

$$W=\frac{Rw_0w_2e^{-B_{iv}/k\theta}}{w_2-Rw_0e^{-B_{iv}/k\theta}}, \tag{47}$$

where $R=f_0[D_{\text{Zn}}^*/D_{\text{Al}}(0)]$. Within experimental error the ratio $D_{\text{Zn}}^*/D_{\text{Al}}(0)$ (Refs. 27 and 29) is independent of temperature and has a value lying between 2.0 and about 7.3. [The uncertainty arises from difficulty in relating $1/\tau_{\text{Al}}(0)$ to $D_{\text{Al}}(0)$; a value near 2.0 is favored by other results on pure Al.] From Eqs. (43) and (44) with $c=0$, we know w_2 and w_0, apart from the constants K_2 and K_0. However, a relation between K_2 and K_0 can be found from the requirement on Eq. (47) that

$$w_2\geq Rw_0e^{-B_{iv}/k\theta} \tag{48}$$

for a physically reasonable result ($W>0$). Choosing $D_{\text{Zn}}^*/D_{\text{Al}}(0)=2.0$, and $f_0=0.78$, Eq. (48) leads to the condition that K_2/K_0 must be $\lesssim 0.37$ over our experimental range of temperature, and for $B_{iv}=0.19$ eV. Now the product K_2W can be found as a function of temperature for any choice of $R(K_2/K_0)$ that satisfies (48), and from this f is determined from Eq. (45) as a function of both temperature and $R(K_2/K_0)$. We find, independently of our choice of $R(K_2/K_0)$, that f is a

[31] Steven J. Rothman and Norman L. Peterson (private communication).

strong function of temperature which is well described over our experimental temperature range by a single exponential in $-1/\theta$. The temperature dependence of f yields an activation energy that is, for any reasonable value of RK_2/K_0, approximately 0.47 eV$=E_{C.F.}$. With this we are able to compare our result with that of the tracer measurement. Since $D_{Zn}{}^*=D_{0Zn}{}^* \exp(-Q_{Zn}{}^*/k\theta)$ $=D_{0Zn}{}^* w_2 f \exp[(-E_f+B_{iv})/k\theta]$, then

$$Q_{Zn}{}^*=E_{m2}+E_{C.F.}+E_f-B_{iv}=1.25 \text{ eV}$$

as required. We conclude that $w_2 \gg W$ over almost the entire range of temperature; W varies approximately as $\exp(-0.68 \text{ eV}/k\theta)$ over this same range, suggesting that (if $w_1 > \frac{7}{2} F w_3$) $E_{m1}=0.68$ eV. Under these circumstances the Al atoms jumping in the vicinity of the impurity provide the rate controlling factor in $D_{Zn}{}^*$; while the impurity jump rate dominates the nuclear relaxation process.

Preliminary isotope effect results of Rothman and Peterson[31] indicate a value of $f \approx 0.6$ and a small temperature dependence. The large temperature dependence of f found above may indicate a breakdown in the linear theory of alloy diffusion we have employed, especially in view of the possible effects of clustering in our alloys. This possibility requires further attention.

We have consciously employed two inconsistent assumptions in formulating the analysis in this paper. Clearly a long-range interaction is required, and is proper, to describe the quadrupolar effects, yet we use the assumption for a vacancy-impurity pair of a binding energy B_{iv} which falls to zero beyond the nearest neighbor. This is conventional in diffusion studies and statistical treatments of solid solutions; but the juxtaposition of these two working assumptions within a single study emphasizes the disparity.

Two previous extensive nuclear magnetic resonance studies of aluminum alloys have been reported.[32,33] Each of these used the steady-state technique to observe the parameters of the Al^{27} absorption in concentrated Al alloys as a function of temperature; their objectives were rather different from ours. The work of Webb[32] was largely concerned with the size of the mean-square electric-field gradient over all nuclei, such as we use in $\tilde{H}_Q{}^2$. Insofar as the quantities discussed are comparable, they are consistent; we have been rather more concerned about $H_Q{}^2$, which pertains only to those nuclei in spin-temperature equilibrium. Regarding the work of Stoebe *et al.*,[33] the quantity Q which they extract from their data is primarily a measure of the Al jump rate, and as such is consistent with our view of this quantity. It varies only slightly among the alloys we investigated, all of which were more dilute than their least dilute. We agree with their assertion that the jump frequency of Zn is very much greater than that of Al, although our arguments differ substantially from theirs. Our conclusions are also consistent with the results of tracer measurements done by Hilliard *et al.*,[34] a discussion of which has been given by Stoebe.

V. CONCLUSIONS

The results of Sec. IVA provide verification of the hypothesis of a spin temperature in the rotating frame in the presence of an inhomogeneous quadrupole interaction in Al alloys. For the alloys studied the local field is shown to be composed of two terms: The dipolar term is independent of solute addition; the quadrupolar term has a concentration dependence which is explained in terms of the mean-square electric field gradient at an Al nucleus in spin temperature equilibrium.

The results presented in Sec. IV B verify the need to consider both the dipolar and quadrupolar contributions to relaxation in order to explain the concentration and temperature dependence of $T_{1\rho}$ in Al alloys. The contribution to the relaxation rate due to the fluctuating nuclear electric quadrupole interaction enables one to derive information about intrinsic solute jump rates. This information, when accompanied by knowledge of excess vacancy concentration, provides an improved understanding of diffusion in dilute alloys.

ACKNOWLEDGMENT

We would like to thank Dr. Norman Peterson for helping us to clarify the arguments relating our results to tracer studies.

[32] M. B. Webb, J. Phys. Chem. Solids **20**, 127 (1961).
[33] T. G. Stoebe, R. D. Gulliver, II, T. O. Ogurtani, and R. A. Huggins, Acta Met. **13**, 701 (1965).
[34] J. E. Hilliard, B. L. Averbach, and Morris Cohen, Acta Met. **7**, 86 (1959).